

# 福島県立医科大学 学術機関リポジトリ



Title	Histological distribution and ultrastructural features of immunoreactive terminals against RT97, a monoclonal antibody to a 200 kD neurofilament, in the spinal dorsal horn of a rat
Author(s)	Ishii, Maiko; Miyashita, Tomoko; Tsuchiya, Kaori; Ueda, Kouki; Umemura, Akira; Honda, Takashi
Citation	Fukushima Journal of Medical Science. 50(2): 65-74
Issue Date	2004-12
URL	<a href="http://ir.fmu.ac.jp/dspace/handle/123456789/159">http://ir.fmu.ac.jp/dspace/handle/123456789/159</a>
Rights	© 2004 The Fukushima Society of Medical Science
DOI	10.5387/fms.50.65
Text Version	publisher

This document is downloaded at: 2024-04-18T21:32:10Z

HISTOLOGICAL DISTRIBUTION AND ULTRASTRUCTURAL FEATURES  
OF IMMUNOREACTIVE TERMINALS AGAINST RT97,  
A MONOCLONAL ANTIBODY TO A 200 kD NEUROFILAMENT,  
IN THE SPINAL DORSAL HORN OF A RAT

MAIKO ISHII<sup>1)</sup>, TOMOKO MIYASHITA<sup>1)</sup>, KAORI TSUCHIYA<sup>1)</sup>,  
KOUKI UEDA<sup>1)</sup>, AKIRA UMEMURA<sup>1)</sup> and TAKASHI HONDA<sup>2)</sup>

<sup>1)</sup>Fukushima Medical University School of Medicine, Student

<sup>2)</sup>Department of Anatomy II, Fukushima Medical University School of Medicine, Fukushima

(Received September 8, 2004, accepted October 13, 2004)

**Abstract :** Localization and ultrastructural features of immunoreactive fibers and terminals against RT-97, a mouse monoclonal antibody that recognizes subunit of a 200-kD neurofilament, were examined in the spinal dorsal horn of adult rats. Under a light-microscope, many RT-97 immunoreactive fibers were detected in the dorsal root, collaterals of the dorsal root in the dorsal funiculus, and laminae III and IV in the dorsal horn. Few immunoreactive fibers were found in laminae I and II. Electron microscopic observation demonstrated that almost all RT-97 immunoreactive fibers in the dorsal root were myelinated, and unmyelinated fibers immunonegative. The immunoreactive fibers entered into the dorsal horn passing through the collaterals of the dorsal root along the superficial gray lamina. In the dorsal horn, these fibers ascended into and then terminated in lamina II. RT-97 immunoreactive central terminals were semicircular or ellipsoid in appearance and contained many flat-type presynaptic vesicles. Some terminals made synaptic contact with dendritic profiles in lamina II.

Our present results indicate that RT-97 is a useful marker for ultrastructural examination of terminals served by non-nociceptive A-fibers.

**Key words :** non-nociceptive A-fibers, central terminals, synapses, flat vesicles, spinal cord

---

石井舞子, 宮下朋子, 土屋 香, 植田航希, 梅邑 晃, 本多たかし  
Correspondence to : Takashi Honda, Department of Anatomy II, Fukushima Medical University School of Medicine, Fukushima City 960-1295, Japan.  
E-mail : ponchan@fmu.ac.jp

## INTRODUCTION

RT 97 is a monoclonal antibody that specifically binds to a 200 kD neurofilament protein. Early immunohistochemical studies in the dorsal root ganglion demonstrated that this protein localizes in the large ganglion neurons that mainly projected and terminated in laminae III and VI of the spinal dorsal horn<sup>1-6)</sup>. It is well established that laminae III and VI of the spinal dorsal horn receives sensory information from peripheral low-threshold mechanoreceptors. Although early evidence strongly suggested that understanding of the ultrastructural features of RT97 immunoreactive terminals might be important in elucidating the sensory mechanisms in the spinal dorsal horn, we still have little information on this. In the present study, therefore, we attempted to demonstrate the fine structures of RT 97 immunoreactive terminals distributed in the spinal dorsal horn of a rat. In addition, we examined the synaptic organization in the spinal dorsal horn of a rat electron-microscopically. Based on these results, we discuss the physiological roles of RT 97 immunoreactive terminals in the synaptic organization of the spinal dorsal horn. Our present results may contribute to a deeper physiological and morphological understanding of spinal sensory mechanisms.

## MATERIALS AND METHODS

*Experimental animals*

A total of 6 male Wistar rats were used. All animal experiments in the present study conformed to the regulations of the Animal Research Committee of Fukushima Medical University in accordance with the Guidelines on Animal Experiments at Fukushima Medical University and Japanese Government Animal Protection and Management Law (No. 105).

*Ultrastructure of synaptic organization in substantia gelatinosa of a rat*

Three male Wistar rats, 15 weeks old and weighing around 250 g, were used in this experiment. Rats were anesthetized with sodium pentobarbital (Nembutal, 50 mg/kg i.p., Dainihon Seiyaku) and transcardially perfused with 350 ml of 0.1% heparinized saline, followed by the same volume of fixative containing 2% glutaraldehyde in 0.1 M phosphate buffer (GA). After perfusion, the lumbar spinal cord was removed from the spine and post-fixed with GA for 2 h at room temperature. The spinal cord was then embedded in 4% gelatin and cut on a vibrating microtome (Microslicer, D.S.K.) into 200  $\mu\text{m}$  serial coronary sections. Sections were post-fixed with GA overnight and osmified with 1% osmium tetroxide in 0.1 M phosphate buffer for 2 h. After osmication, sections were processed through conventional dehydration using an ascending series of ethanol, followed by acetone. Finally, each section was flat-embedded with epoxy resin (Epon 812, TAAB) on a resin block prepared in

advance. Resin was polymerized in an oven at 80°C for 5 days. Then, 1  $\mu\text{m}$  thick sections were cut on an ultramicrotome (MT6000, RMC) and stained with 1% toluidine blue for preliminary observation on a light microscope. For light microscopic observation of the toluidine blue stained sections, a region containing laminae II, III and VI was trimmed on an embedded block. Ultra-thin sections were cut and double-stained with uranyl acetate and lead citrate. Finally, sections were examined on an electron microscope (JEM1200EX, JEOL) at 80 kV of an accelerating voltage. Fine structure of laminae II, III and VI was photographed at random at a magnification of X 25,000.

#### *RT97 immunohistochemistry & immunoelectron microscopy*

Three male Wistar rats, weighing 250 g at 15 weeks old, were anesthetized with sodium pentobarbital (Nembutal, 50 mg/kg, i.p.) and transcardially perfused with 350 ml of 0.1% heparinized saline, followed by the same volume of fixative containing 4% paraformaldehyde in 0.1 M phosphate buffer (PFA). The cervical, thoracic and lumbar spinal cord were removed and immersed in PFA for 2 h at room temperature. Each part of the spinal cord was then separated into two blocks. One block was dehydrated with immersion in 20% sucrose solution, and rapidly frozen at -80°C. The frozen tissues were cut on a cold microtome (Yamato-Koki, Japan) into serial 50  $\mu\text{m}$  sections. The other block was embedded in 4% gelatin and cut on a vibrating microtome (Microslicer, D.S.K., Japan) into serial 100  $\mu\text{m}$  coronary sections. The frozen sections were used for light microscopic immunohistochemical examination, and the vibratome sections for immunoelectron microscopy.

Immunohistochemical staining for RT97 was performed on free-floating sections. After rinsing with 10 mM phosphate buffered saline (PBS), sections were reacted in a solution containing anti-200 kD neurofilament mouse IgG (RT97, Chemicon) at a dilution of 1 : 1,000 in PBS for 48 h at 4°C. Peroxidase was combined with the primary antibodies by the avidine and biotin-peroxidase complex (ABC) method. The binding sites of the antibodies were made visible with the enzyme-histochemical technique for peroxidase using 3, 3' diaminobenzidine dihydrochloride (DAB) as a chromogen. After staining, cold-microtome sections were mounted on a glass slide coated with silane, dried at room temperature and coverslipped.

In the spinal dorsal horn, distribution of immunoreactive structures was traced by a camera-lucida drawing tube attached to a light microscope. The number of immunoreactive fibers and area of each lamina in the dorsal horn were calculated on exactly traced figures by three examiners. The fiber density of each lamina was expressed by the mean value of the number of immunoreactive fibers in a lamina.

For immunoelectron microscopy, post-immunostained microslicer sections were post-fixed with 2% GA overnight, and then embedded with plastic resin (Epon 812, TAAB) by processing according to the same procedure as used for conventional electron microscopy.

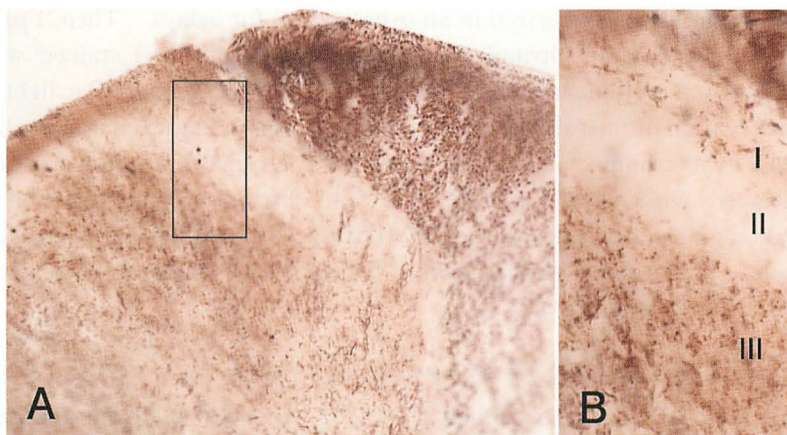


Fig. 1. Light-micrographs of RT-97 immunoreactive structures in the dorsal horn of the rat spinal cord. High-power magnified view of the rectangle in A is shown in B. Roman numerals in B indicate lamina in the dorsal horn.

## RESULTS

### *Distribution of RT97 immunoreactive fibers in the spinal dorsal horn of a rat*

On light microscopic observation, RT97 immunoreactive structures were recognized as a deposition of dark brownish colored reaction products and easily distinguished from immunonegative structures. RT-97 immunoreactive fibers were found in the dorsal root, the dorsal funiculus containing the fasciculus gracilis and the fasciculus cuneatus, the lateral funiculus containing the posterior spinocerebellar tract and the lateral corticospinal tract. A noteworthy finding was that thick bundles of immunoreactive fibers were found in the collaterals of dorsal root fibers, detouring along the superficial inside of the dorsal horn (Fig. 1 and 2). Many immunoreactive fibers entered into the dorsal horn passing through the region of the intermedial basis of the dorsal horn, which resulted in a high density of immunoreactive fibers in laminae III and IV (Fig. 2). A few immunoreactive fibers in the dorsal root directly entered into the dorsal horn passing through the zone of Lissauer.

### *Synaptic organization of laminae III and IV in spinal dorsal horn of a rat*

Central terminals distributed in laminae II, III and IV were divided into following two groups: one in which the terminals contained round synaptic vesicles and one in which the terminals contained flat synaptic vesicles (Fig. 3). The ratio of the longer to the shorter axis (LS ratio) was measured in each vesicle. In this experiment, we regarded a synaptic vesicle showing an LS ratio of less than 2 to be vesicles of the round type. Vesicles showing an LS ratio of more than 2 were regarded as flat type (flat vesicle: FV). Round vesicles were further divided into three sub-

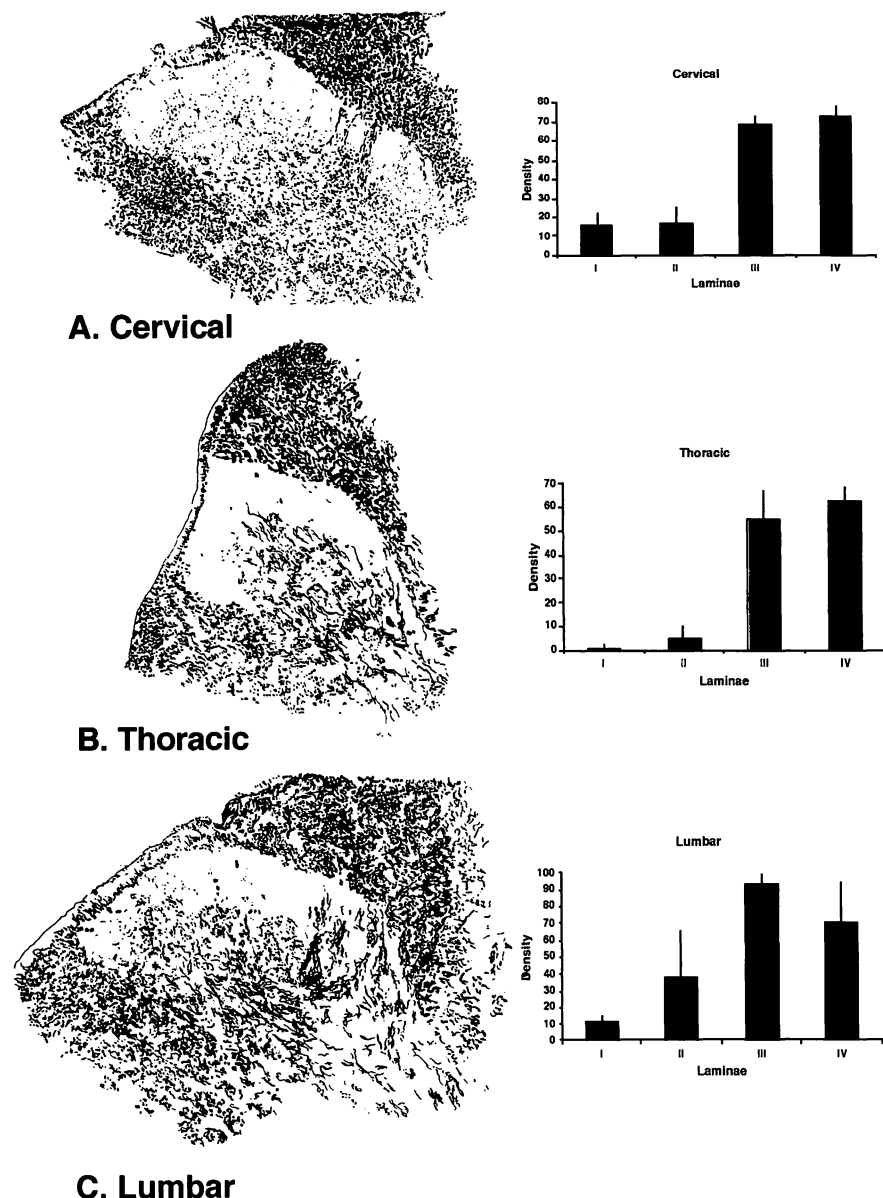


Fig. 2. Camera-Lucida drawings of RT-97 immunoreactive fibers in various levels of the spinal cord (C2, Th9 and L2). Graphs in the right column indicate density of RT-97 immunoreactive fibers in each level of the spinal cord shown in the left column.

groups: small vesicles of less than 75 nm in diameter (small round: SR), large round vesicles of more than 75 nm (large round: LR) and large granular vesicles having a dense core (large granular vesicle: LGV). Furthermore, small round vesicles were divided into the following two subgroups on the basis of the cytoplasmic density in

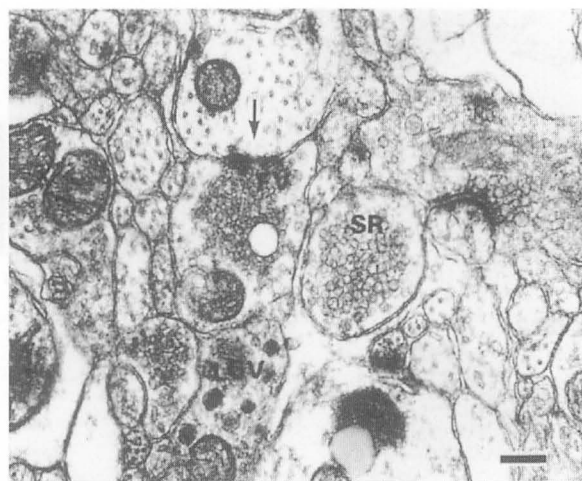


Fig. 3. Various types of terminal in lamina II. Terminals containing small round vesicles (SR), flat vesicles (FV) and large granular vesicles (LGV) are seen. A terminal containing flat vesicles makes an asymmetric synaptic contact with a dendrite (arrow).

Scale bar indicates 200 nm.

Table 1. Variation of terminals in lamina II of the spinal dorsal horn of a rat.

Vesicle appearance	Cytoplasmic density	Number of terminals	% of types
Small round	low	1,264	77.5
	high	35	2.1
Large round		42	2.6
Large granular		63	3.9
Flat		228	14.0
Total		1,632	100.0

terminals. One group had small round vesicles in electron-dense cytoplasm (small round, high density; SRH), and the other small round vesicles in low density cytoplasm (small round, low density; SRL). In 1,632 terminals, the majority of vesicles were RSL or FV type, at 77.5 % and 14.0 %, respectively. Conversely, SRH, LR and LGV had small populatione (SRH, 2.1% ; LR, 2.6% ; LGV, 3.9% ; data shown in Table 1). Almost all of these terminals formed axo-dendritic synapses with dendritic profiles in the inner layer of lamina II (Fig. 3).

#### *Ultrastructure of RT97 immunoreactive structures in the spinal dorsal horn*

In the electron microscopic observation, immunoreactivity against RT-97 was identified by deposition of osmified DAB reaction products showing high electron-density, and easily distinduished from immunonegative structures. In the present results, almost all myelinated thick axons showed RT-97 immunoreactivity and

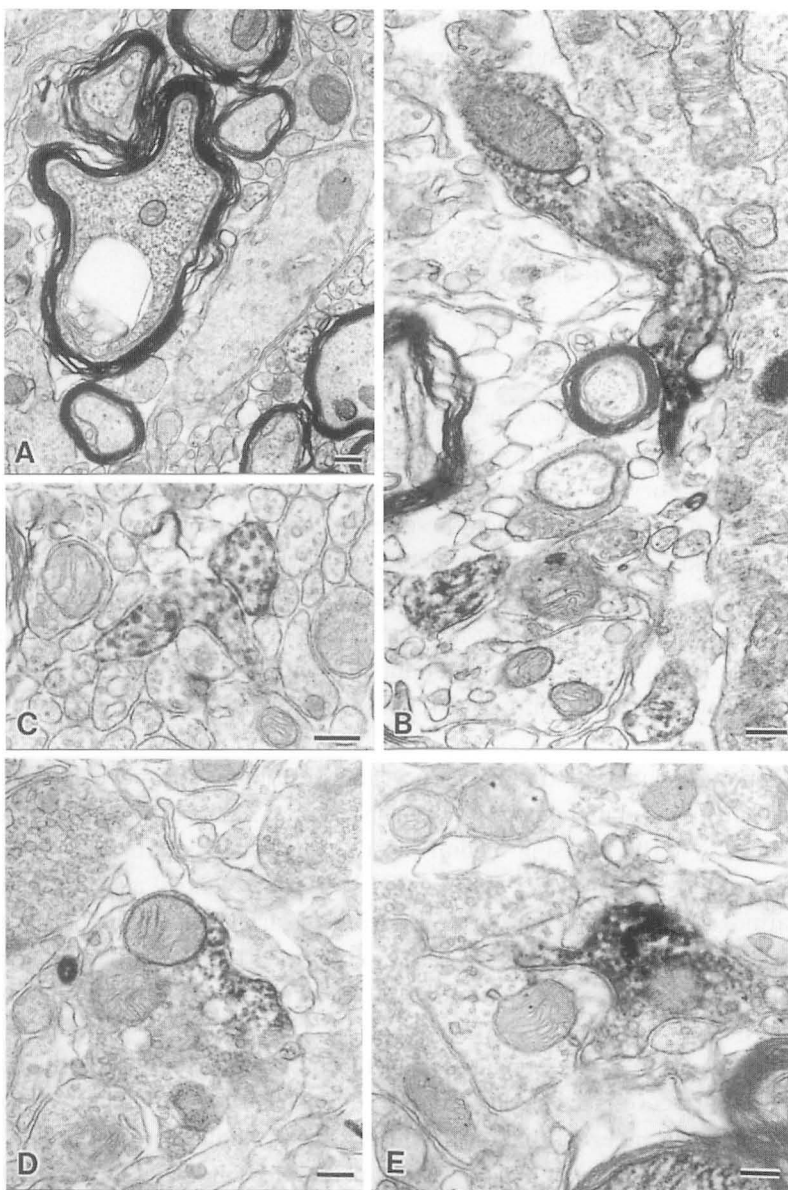


Fig. 4. Ultrastructural features of RT-97 immunoreactive fibers that enter into the dorsal horn intermingled among collaterals of dorsal root fibers (A). All RT-97 immunoreactive fibers are myelinated. Unmyelinated fibers were immunonegative.

In laminae III and IV, immunoreactive fibers lost their myelin sheath (B). Small spine-like structures also showed immunoreactivity (C). RT-97 immunoreactive terminals in the outer layer of lamina III and inner layer of lamina II (D, E) contain many synaptic vesicles of flat type appearance.

All scale bars in this figure indicate 200 nm

unmyelinated fibers were immunonegative in the dorsal root (Fig. 4A). In the deep layer of the dorsal horn, lamina III and IV, these immunoreactive fibers lost their myelin sheath and showed terminal profiles (Fig. 4B). Small immunoreactive structures, regarded as axonal spines, were intermingled in the neuropil of laminae III (Fig. 4C). In the upper layer of lamina III and the inner layer of lamina II, RT-97 immunoreactive fibers formed terminal buttons that commonly contained synaptic vesicles of the flat type (Fig. 4D, E). Some of these synaptic buttons made synaptic contact with dendritic profiles in lamina II (Fig. 4E).

#### DISCUSSION

Morphological and physiological studies have suggested that immunoreactivity against RT-97 is localized in myelinated fibers in the peripheral nervous system of both adult and embryo<sup>2-5)</sup>. In the central nervous system, RT-97 also recognized thick myelinated fibers<sup>6)</sup>. Although these results strongly suggest that RT-97 might be a useful marker for myelinated A-fibers, we have currently little information on ultrastructural aspects of RT-97 immunoreactive fibers. In the present study, we demonstrated ultrastructurally that almost all RT-97 immunoreactive fibers projecting to the superficial layer of the spinal dorsal horn were myelinated, and that RT-97 immunoreactivity was mainly found in the central terminals containing flat-type synaptic vesicles.

It is generally understood that the central projection of non-nociceptive primary afferents is myelinated and enters into the spinal cord as part of the medial division of root fibers by either passing medial to or through the superficial gray laminae. These larger caliber fibers enter into lamina II from its ventral aspect and arborize near gelatinous neurons, in relation to dendrites of large cells of the proper sensory nucleus in lamina IV<sup>7)</sup>. Our present results confirmed that RT-97 immunoreactive fibers are distributed in an area similar to the projection pathway of these non-nociceptive primary afferents.

The dorsal horn of the spinal cord is the first region of interaction between primary afferent neurons projecting from the dorsal root ganglion via the dorsal root and spinal intrinsic neurons having a variety of ascending projections to higher neuronal centers. In morphological studies performed on spinal cord structures of the cat, rat<sup>8)</sup>, and the primate<sup>9)</sup>, synaptic profiles in the dorsal horn have been classified into several subtypes according to the synaptic vesicles, basically consisting of round vesicles, flat vesicles and large granular vesicles. In the present study, we obtained similar results to these early studies. Our present results also indicated that RT-97 immunoreactive terminals contained synaptic vesicles with flat type appearance. Recently, the synaptic organization of nociceptive primary afferents has been investigated in the spinal dorsal horn<sup>10,11)</sup>. Immunohistochemical technique has contributed to these ultrastructural investigations, since immunoreactivity for several kinds of neuropeptides is regarded as a useful marker to identify primary

afferent C fibers<sup>12-17</sup>. Pickel *et al.* reported that immunoreactivity against substance P was selectively associated with large (60-80 nm), round vesicles<sup>18</sup>. It is generally recognized that substance P immunoreactive terminals in lamina II are served by nociceptive afferent C-fibers. On the other hand, we still have little information on the synaptic features of non-nociceptive primary afferents in the superficial layer of the dorsal horn that originate mainly from large neurons in the dorsal root ganglion, perhaps because we have no useful marker to identify both thick myelinated fibers and their terminals. Although carbonic anhydrase activity has been used as such a marker, it can't recognize only large non-nociceptive afferent neurons in the dorsal root ganglion<sup>19-23</sup>. Our present results indicate that RT-97 may be a useful tool for ultrastructural examination of terminals served by non-nociceptive A-fibers in the dorsal horn.

Woolf et al have provided interesting evidence that the central terminals of axotomized myelinated-affersents, ordinarily terminated in laminae III and IV of the spinal cord, sprout into lamina II, which has an important role in the modulation of pain sensation<sup>24</sup>. This strongly suggests that changes in synaptic organization in the superficial layer of the dorsal horn might have a key role in the onset mechanism of allodynia in neuropathic pain. We therefore need a useful maker for terminals served by non-nociceptive A-fibers in the dorsal horn. The present findings suggest that mouse monoclonal antibody RT-97, which recognizes the 200-kDa neurofilament subunit, selectively labeled terminals served by sensory myelinated A-fibers in the spinal dorsal horn. This should contribute to the study of the morphological aspects of synaptic organization in the dorsal horn.

#### ACKNOWLEDGEMENTS

The authors thank Ms. Atsuko Yabashi and Mr. Katsuyuki Kanno for their excellent technical assistance, and Prof. Naonori Sugai MD, PhD for a critical reading of an early version of this manuscript.

#### REFERENCES

1. Kai-Kai MA. Cytochemistry of the trigeminal and dorsal root ganglia and spinal cord of the rat. *Comp Biochem Physiol A-Comp Physiol*, **93**(1): 183-193, 1989.
2. Jackman A, Fitzgerald M. Development of peripheral hindlimb and central spinal cord innervation by subpopulations of dorsal root ganglion cells in the embryonic rat. *J Comp Neurol*, **418**(3): 281-298, 2000.
3. Sann H, McCarthy PW, Jancso G, Pierau FK. RT 97: a marker for capsaicin-insensitive sensory endings in the rat skin. *Cell Tissue Res*, **282**(1): 155-161, 1995.
4. McCarthy PW, Petts P, Hamilton A. RT97- and calcitonin gene-related peptide-like immunoreactivity in lumbar intervertebral discs and adjacent tissue from the rat. *J Anat*, **180** (Pt 1): 15-24, 1992.
5. Hall SM, Kent AP, Curtis R, Robertson D. Electron microscopic immunocytochemistry of GAP-43 within proximal and chronically denervated distal stumps of transected

- peripheral nerve. *J Neurocytol*, **21**(11) : 820-831, 1992.
- 6. Sbarbati A, Bunnemann B, Cristofori P, Terron A, Chiamulera C, Merigo F, Benati D, Bernardi P, Osculati F. Chronic nicotine treatment changes the axonal distribution of 68 kDa neurofilaments in the rat ventral tegmental area. *Eur J Neurosci*, **16**(5) : 877-882, 2002.
  - 7. Carpenter MB. Spinal cord: Regional anatomy and internal structure. In: Carpenter's Human Neuroanatomy. 9th ed. Williams & Wilkinson, Baltimore, 325-367, 1996.
  - 8. Kerr FWL. Neuroanatomical substrates of nociception in the spinal cord. *Pain*, **1** : 325-356, 1975.
  - 9. Ralston III HR. The fine structure of laminae I, II and III of the macaque spinal cord. *J Comp Neurol*, **184** : 619-642, 1979.
  - 10. Ma W, Peschanski M. Spinal and trigeminal projections to the parabrachial nucleus in the rat: electron-microscopic evidence of a spino-ponto-amygdkalian somatosensory pathway. *Somatosens Res*, **5**(3) : 247-257, 1988.
  - 11. Cuello AC, Priestley JV, Matthews MR. Localization of substance P in neuronal pathways. *Ciba Foundation Symposium*, **91** : 55-83, 1982.
  - 12. Lazarov NE. Comparative analysis of the chemical neuroanatomy of the mammalian trigeminal ganglion and mesencephalic trigeminal nucleus. [Review] *Prog Neurobiol*, **66**(1) : 19-59, 2002.
  - 13. Alvarez FJ, Fyffe RE. Nociceptors for the 21st century. *Curr Rev Pain*, **4**(6) : 451-458, 2000.
  - 14. Maxwell DJ, Kerr R, Jankowska E, Riddell JS. Synaptic connections of dorsal horn group II spinal interneurons: synapses formed with the interneurons and by their axon collaterals. *J Comp Neurol*, **380**(1) : 51-69, 1997.
  - 15. Cheng PY, Moriwaki A, Wang JB, Uhl GR, Pickel VM. Ultrastructural localization of mu-opioid receptors in the superficial layers of the rat cervical spinal cord: extrasynaptic localization and proximity to Leu5-enkephalin. *Brain Res*, **731**(1-2) : 141-154, 1996.
  - 16. Blomqvist A, Ericson AC, Craig AD, Bromann J. Evidence for glutamate as a neurotransmitter in spinothalamic tract terminals in the posterior region of owl monkeys. *Experimental Brain Res*, **108**(1) : 33-44, 1996.
  - 17. Sommer C, Myers RR. Neurotransmitters in the spinal cord dorsal horn in a model of painful neuropathy and in nerve crush. *Acta Neuropathol*, **90**(5) : 478-485, 1995.
  - 18. Pickel VM, Reis DJ, Leeman SE. Ultrastructural localization of substance P in neurons of rat spinal cord. *Brain Res*, **122** : 534-540, 1977.
  - 19. Perry MJ, Lawson SN. Differences in expression of oligosaccharides, neuropeptides, carbonic anhydrase and neurofilament in rat primary afferent neurons retrogradely labelled via skin, muscle or visceral nerves. *Neuroscience*, **85**(1) : 293-310, 1998.
  - 20. Zheng F, Lawson SN. Immunocytochemical properties of rat renal afferent neurons in dorsal root ganglia: a quantitative study. *Neuroscience*, **63**(1) : 295-306, 1994.
  - 21. Sugimoto T, Takemura M, Ichikawa H, Akai M. Carbonic anhydrase activity in the trigeminal primary afferent neuronal cell bodies with peripheral axons innervating the mandibular molar tooth pulps of the rat. *Brain Res*, **505**(2) : 354-357, 1989.
  - 22. Robertson B, Grant G. Immunocytochemical evidence for the localization of the GM1 ganglioside in carbonic anhydrase-containing and RT 97-immunoreactive rat primary sensory neurons. *J Neurocytol*, **18**(1) : 77-86, 1989.
  - 23. Peyronnard JM, Charron L, Lavoie J, Messier JP, Dubreuil M. Carbonic anhydrase and horseradish peroxidase: double labelling of rat dorsal root ganglion neurons innervating motor and sensory peripheral nerves. *Anat Embryol*, **177**(4) : 353-359, 1988.
  - 24. Woolf CJ, Shortland P, Coggeshall RE. Peripheral nerve injury triggers central sprouting of myelinated afferents. *Nature*, **355**(6355) : 75-78, 1992.